Published in final edited form as:
Acta Biomater. 2014 January ; 10(1): . doi:10.1016/j.actbio.2013.09.004.

Dual-crosslinked oxidized, methacrylated alginate/PEG hydrogels for bioadhesive applications

Oju Jeon[a], **Julia E. Samorezov**[a], and **Eben Alsberg**[a,b,c,*]

[a]Department of Biomedical Engineering, Case Western Reserve University, Cleveland, OH 44106, USA

[b]Department of Orthopaedic Surgery, Case Western Reserve University, Cleveland, OH 44106, USA

[c]Division of General Medical Sciences, National Center for Regenerative Medicine, Case Western Reserve University, Cleveland, OH 44106, USA

Abstract

A degradable, cytocompatible bioadhesive can facilitate surgical procedures and minimize patient pain and postsurgical complications. In this study, a bioadhesive hydrogel system based on oxidized, methacrylated alginate/8-arm poly(ethylene glycol) amine (OMA/PEG) has been developed, and the bioadhesive characteristics of the crosslinked OMA/PEG hydrogels are evaluated. Here, we demonstrate that the swelling behavior, degradation profiles, and storage moduli of crosslinked OMA/PEG hydrogels are tunable by varying the degree of alginate oxidation. The crosslinked OMA/PEG hydrogels exhibit cytocompatibility when cultured with human bone marrow-derived mesenchymal stem cells. In addition, the adhesion strength of these hydrogels, controllable by varying the alginate oxidation level and measured using a porcine skin model, is superior to commercially available fibrin glue. This OMA/PEG hydrogel system with controllable biodegradation and mechanical properties and adhesion strength may be a promising bioadhesive for clinical use in biomedical applications, such as drug delivery, wound closure and healing, biomedical device implantation, and tissue engineering.

Keywords

bioadhesive; alginate; PEG; biodegradation; adhesion

1. Introduction

Bioadhesion, where natural and synthetic materials adhere to biologic tissues such as skin or mucous membranes, is a valuable property that can be exploited clinically, including in wound closure and healing, drug delivery, implantation of biomedical devices, tissue engineering, and dental and bone applications [1–4]. Bioadhesives are natural or synthetic materials that can be used for soft tissue repair to create a seal preventing leakage of biological fluids or to reinforce anatomic integrity as an attractive alternative to sutures and

*Corresponding author Tel.: +1 216 368 6425; fax: +1 216 368 4969. eben.alsberg@case.edu (E. Alsberg).

staples [5]. The most widely used bioadhesives are fibrin, cyanoacrylates, and albumin-glutaraldehyde bioadhesives [5]. Fibrin bioadhesive, which is formed by mixing fibrinogen and thrombin and commercially available as Tisseel® (Baxter, Westlake Village, CA) and Hemaseel (Hemacure, Sarasota, FL), is the most widely used surgical bioadhesive in clinical practice because it is biodegradable and biocompatible [6]. However, fibrin bioadhesive exhibits relatively weak adhesion to tissues and fast degradation compared to cyanoacrylate and albumin-glutaraldehyde bioadhesives [7]. In addition, there is the risk of viral disease transmission, since fibrinogen is obtained from human plasma [8]. Cyanoacrylate (Dermabond, Ethicon Inc., Somerville, NJ) is a synthetic bioadhesive that polymerizes in the presence of body fluids [9]. Although cyanoacrylates have performed satisfactorily in many clinical applications, they form solid impermeable polymers which release formaldehyde that can cause an inflammatory response and local tissue necrosis [10]. Albumin-glutaraldehyde bioadhesive (BioGlue, CryoLife Europa, Hampshire, United Kingdom) has also been used in surgical procedures after it was shown to aid in achieving hemostasis around sutures or staples in large blood vessels [5]. Although albumin-glutaraldehyde bioadhesive exhibits strong adhesion strength to tissues and biomaterials, it can cause significant problems in vivo, such as edema, an inflammatory response, and tissue necrosis [11].

Recently, oxidized polysaccharide bioadhesives comprised of dextran [12], alginate [13, 14], chondroitin sulfate [15, 16], and starch [17] have been developed to try to address aforementioned disadvantages in commercial bioadhesives. These bioadhesives are biodegradable and biocompatible, and exhibit relatively strong adhesion to tissues when compared to fibrin bioadhesive. The mechanical properties and adhesion strength of these materials could be varied with oxidation level to achieve tissue-specific bioadhesives. As the oxidation level of polysaccharides increased, the modulus and adhesion strength of many of the bioadhesives increased [12, 14, 17, 18] due to the greater number of reactive aldehyde groups available for crosslinking. However, higher degrees of polysaccharide oxidation result in rapid degradation that might be unsuitable for most in vivo bioadhesive applications as rapid degradation can lead to loss of adhesion capacity and mechanical stability of bioadhesives [18]. An ideal bioadhesive would allow for rapid and robust adhesion to maintain wound integrity during biological healing processes, and ease of handling to permit application in a precisely controlled manner. Additionally, the bioadhesive should be biocompatible and have the potential of tailorable mechanical and biodegradation properties to match the needs of organ and/or tissue-specific applications [19–21].

The purpose of this study was to engineer a dual-crosslinked oxidized, methacrylated alginate/8-arm poly(ethylene glycol) amine (OMA/PEG) hydrogel system as a bioadhesive with controllable mechanical properties, adhesion strength and biodegradation rate. Alginate was chemically functionalized with aldehyde groups by oxidation to react with amine groups of PEG, and then a fraction of the alginate's carboxylic acids were further modified with 2-aminoethylmethacrylate (AEMA) via carbodiimide chemistry [22] to allow photocrosslinking of the methacrylate groups by ultraviolet (UV) light. The effect of varying the degree of alginate oxidation was evaluated through examination of hydrogel shear moduli, swelling behavior, degradation profiles and adhesion strength with porcine skin. The OMA/PEG hydrogel system exhibits cytocompatibility and controllable physical properties. The bioadhesion strength of this system is tunable by varying the alginate oxidation level and superior to commercially available fibrin glue as measured using porcine skin. This dual-crosslinked OMA/PEG bioadhesive hydrogel system with controllable physical properties and bioadhesion strength may be useful for a wide range of clinical applications.

2. Materials and methods

2.1. Preparation of OMA and 8-arm PEG-amine

The OMA macromers were prepared as previously described [22]. Briefly, to prepare the oxidized alginate, sodium alginate (20 g, Protanal LF 20/40, 196,000 g/mol, FMC Biopolymer, Philadelphia, PA) was dissolved in ultrapure deionized water (diH_2O, 1800 ml). Sodium periodate (2, 3.5 and 5 g, Sigma, St. Louis, MO) was dissolved in 200 ml diH_2O and added into separate alginate solutions to achieve different degrees of theoretical alginate oxidation (10, 17.5, and 25 %) under stirring in the dark at room temperature. The oxidation was stopped after 24 hrs by addition of ethylene glycol (molar ratio of ethylene glycol:sodium periodate =1:1, Sigma). The oxidized alginate was purified by dialysis (MWCO =3500, Spectrum Laboratories Inc., Rancho Dominguez, CA) against diH_2O for 3 days, filtered (0.22 μm filter, Fisher Scientific, Pittsburgh, PA), and lyophilized. To prepare OMAs at theoretical methacrylation of 45 %, oxidized alginate (10 g) was dissolved in 50 mM 2-morpholinoehtanesulfonic acid (Sigma) buffer solution (1000 ml, pH 6.5) containing 0.5 M NaCl (Fisher). N-hydroxysuccinimide (2.65 g, Sigma) and 1-ethyl-3-(3-dimethylaminopropyl)-carbodiimide hydrochloride (8.75 g, Sigma) were added to the mixture to activate the carboxylic acids of alginate. After 5 min, AEMA-HCl (3.8 g, Polysciences, Warrington, PA) was added to the solution, and the reaction was maintained in the dark at room temperature for 24 hrs. The reaction mixture was precipitated with the addition of excess acetone, dried in a chemical fume hood, and rehydrated to a 1 % solution in diH_2O for further purification. The OMA was purified by dialysis (MWCO =3500, Spectrum Laboratories Inc.) against diH_2O for 3 days, treated with activated charcoal (5 g/1000 ml, 50–200 mesh, Fisher) for 30 min, filtered (0.22 μm filter) and lyophilized. The OMA was dissolved in deuterium oxide (D_2O, 2 w/v %), and placed in a NMR tube. To analyze the oxidation and methacrylation efficiency of the OMAs, ^{1}H-NMR spectra were recorded on a Varian Unity-300 (300MHz) NMR spectrometer (Varian Inc., Palo Alto, CA, USA) using 3-(trimethylsilyl)propionic acid-d_4 sodium salt (0.05 w/v %) as an internal standard. The actual degrees of oxidation and methacrylation were calculated from ^{1}H-NMR spectra as previously reported [22]. The actual degree of oxidation of the alginates, which was used in a naming code for the different formulations (OMA-9, OMA-14, and OMA-20), was 9 %, 14 %, and 20 %. The actual degree of methacrylation of OMA-9, OMA-14 and OMA-20 was 19 %, 21 % and 25 %, respectively. Eight-arm poly(ethylene glycol)-amine hydrochloric acid salt (PEG/HCl, 20 g, Mw = 10,000 Da, Jenkem Technology USA Inc., Allen, TX) was dissolved in 100 ml methylene chloride, and triethylamine (the mole ratio of triethylamine to HCl of PEG/HCl = 2) was added into the PEG solution in order to remove HCl salt from the PEG/HCl. After 24 hrs, the solution was precipitated into an excess of hexanes (Fisher), dried in a chemical fume hood, and rehydrated to a 10 % (w/v) solution in diH_2O for further purification. The PEG was purified by dialysis (MWCO 3500; Spectrum Laboratories Inc.) against diH_2O for 3 days, filtered (0.22 μm filter) and lyophilized.

2.2. Determination of gelling time of the single-crosslinked OMA/PEG hydrogels

To examine gelling properties of the OMA/PEG hydrogels, dynamic rheological measurements were performed with a strain-controlled rheometer (AR-2000ex; TA Instruments, New Castle, DE, USA) using a stainless steel cone and plate geometry with 4° cone angle and 20 mm cone diameter. Plate temperature was maintained at 25°C. OMA (20 w/v %) and PEG (40 w/v %) were separately dissolved in Dulbecco's Modified Eagle Medium with low glucose (DMEM, Sigma) with 0.05% w/v photoinitiator (Irgacure-2959, Sigma). A 1 ml syringe containing 250 μl of OMA solution was joined with a Luer-Lok connector to another 1 ml syringe containing an equal volume of PEG solution, and the two solutions were mixed for 30 s. Immediately after mixing, samples were deposited onto the bottom plate of the rheometer. Both the shear storage (G') and loss (G'') moduli were

measured every 6.5 seconds. These measurements were taken at a loading frequency of 1 Hz and strain of 0.2%. Each measurement was performed three times. The gel point was approximated by the G'/G'' crossover time.

2.3. Rheological properties of single- and dual-crosslinked OMA/PEG hydrogels

To fabricate dual-crosslinked OMA/PEG hydrogels, OMA and PEG solutions were prepared as described above. The mixed OMA/PEG solutions were injected between two glass plates separated by 0.75 mm spacers, incubated for 30 min, and then photocrosslinked with 365 nm UV light (Model EN-280L, Spectroline, Westbury, NY) placed on top of the upper plate at ~1 mW/cm^2 for 15 min to form the dual-crosslinked hydrogels. Dual-crosslinked OMA/PEG hydrogel disks were created using an 8 mm diameter biopsy punch and placed in a humidified incubator at 37°C for 30 min. As a comparative group, single-crosslinked OMA/PEG hydrogel disks were also prepared without photocrosslinking.

The rheological properties of the single- and dual-crosslinked OMA/PEG hydrogels were measured in terms of the storage (G') and the loss (G") moduli using a strain-controlled AR-2000ex rheometer (TA Instruments) using an 8 mm diameter stainless-steel parallel plate geometry with a 0.7–0.8 mm gap. Plate temperature was maintained at 25°C. After the 30 min incubation, the measurement was performed using a dynamic frequency sweep test in which a sinusoidal shear strain of constant peak amplitude (0.2 %) was applied over a range of frequencies (0.6–100 rad/sec) (N=3).

2.4. Swelling behavior, degradation, and mechanical property change of the OMA/PEG hydrogels over time

The single- and dual-crosslinked OMA/PEG hydrogel disks were prepared as described above and lyophilized, and dry weights (W_i) were measured. Dried hydrogel samples were immersed in 10 ml of DMEM and incubated at 37°C, and DMEM was replaced every week. At predetermined time points, samples were removed, rinsed with DMEM, and the swollen (W_s) hydrogel sample weights were measured. The swelling ratio (Q) was calculated by $Q = W_s/W_i$ (N=3 for each time point). After weighing the swollen hydrogel samples, the samples were lyophilized and weighed (W_d). The percent mass loss was calculated by $(W_i - W_d)/W_i \times 100$ (N=3 for each time point).

The dual-crosslinked OMA/PEG hydrogel disks were prepared and incubated as described above. At predetermined time points, the swollen dual-crosslinked OMA/PEG hydrogel disks were punched once again to match the diameter of the parallel plates (8 mm). The storage (G') and loss (G") moduli of the dual-crosslinked OMA/PEG hydrogels were measured using a dynamic frequency sweep test with a strain-controlled AR-2000ex rheometer as described above (N=3 for each time point).

2.5. Cytotoxicity of OMA/PEG mixtures and dual-crosslinked OMA/PEG hydrogels

To evaluate potential cytotoxicity of the OMA and PEG macromers and the dual-crosslinked OMA/PEG hydrogels, an indirect contact methodology was employed. Briefly, a human bone marrow aspirate was harvested from the posterior iliac crest of a donor after informed consent under a protocol approved by the University Hospitals of Cleveland Institutional Review Board. The human bone marrow-derived mesenchymal stem cells (hMSCs) were isolated from the bone marrow aspirate and cultured in the Skeletal Research Center Mesenchymal Stem Cell Facility as previously described [23, 24]. hMSCs (passage number 2) were plated in 6-well tissue culture plates at 1×10^5 cells/well in 3 ml of DMEM containing 10 v/v % fetal bovine serum (FBS, Sigma) and cultured at 37°C and 5 % CO_2 for 24 hrs. Cell culture inserts (25 mm in diameter, 8 μm pore size on PET track-etched membrane; Becton Dickinson Labware Europe, Le Pont De Claix, France) were placed into

each well. To prepared dual-crosslinked OMA/PEG hydrogels for cytotoxicity testing, OMA/PEG mixtures (200 μl, 1:1 volume ratio) were pipetted into 96-well tissue culture plates and photocrosslinked with UV for 15 min. An OMA/PEG mixture (200 μl, 1:1 volume ratio) or a dual-crosslinked OMA/PEG hydrogel was added into each culture insert. hMSCs cultured with a cell culture insert but without the presence of any OMA/PEG mixture or dual-crosslinked hydrogel material were maintained as a comparative group. A control group, not exposed to any OMA/PEG mixture, dual-crosslinked hydrogel material or insert, was maintained in parallel. After 48 hrs incubation, media, inserts and hydrogels were removed. Each well was rinsed with phosphate buffered saline (PBS), and 3 ml of a 20 % CellTiter 96 Aqueous One Solution (Promega Corp., Madison, WI, USA), which contains 3-[4,5-dimethylthiazol-2-yl]-5-[3-carboxymethoxy-phenyl]-2-[4-sulfophenyl]-2H-tetrazolium (MTS-tetrazolium), in PBS was added to each well. The MTS-tetrazolium compound can be metabolized by mitochondria in living cells into a colored formazan product that is soluble in cell culture medium. After incubating at 37°C for 90 min, the absorbance of the solutions was determined at 490 nm using a 96-well plate reader (SAFIRE; Tecan, Austria) (N=5).

2.6. Adhesion strength of OMA/PEG hydrogels

To examine the bioadhesion strength of the hydrogels, porcine hide, with hair removed with a razor blade, was purchased from a local butcher shop and stored at 4°C in Krebs-Ringer bicarbonate buffer solution (Sigma) [25]. Porcine skin tissue samples were cut into rectangular pieces with dimensions of 20×10 mm^2 after removing the subcutaneous layers using a surgical scalpel. As shown in Figure 6A, skin samples were attached to a plastic backing (a PET transparency film) using cyanoacrylate glue (Krazy Glue®, Elmer's Products Inc., Columbus, OH), and their thickness was measured using calipers. After attaching two skin tissue samples with a 1 mm gap, the OMA/PEG mixture (100 μl, volume ratio 1:1) was injected between two tissue specimens and cured in a humidified chamber at room temperature for 2 hrs 45 min after 15 min incubation at atmospheric condition. To compare the adhesion strength of single-crosslinked hydrogels with dual-crosslinked hydrogels, OMA-20/PEG group was photocrosslinked under UV at ~ 1 mW/cm^2 for 15 min, and the dual-crosslinked OMA-20/PEG group was further cured in a humidified chamber at room temperature for 2 hrs 45 min. As a comparative group, a commercially available fibrin bioadhesive (Tisseel®, Baxter Corporation) was prepared according to the manufacturer's instruction. The fibrin bioadhesive (100 μl) was also injected between two tissue specimens, incubated at atmospheric conditions for 15 min, and then cured in a humidified chamber at room temperature for 2 hrs 45 min. The adhesion strength of the bioadhesives was determined by performing constant strain rate tensile tests using a Rheometrics Solid Analyzer (RSAII, Rheometrics Inc., Piscataway, NJ, USA) equipped with a 10 N load cell. The plastic backings were loaded into the clamps of the mechanical tester, the thicknesses of tissue specimens, which were in range of 2.0–4.5 mm, were measured using calipers to calculate cross-sectional areas, and tensile tests were performed on specimens at room temperature using a constant strain rate of 5 %/sec. The adhesion strength is defined as the maximum load force observed in this measurement divided by the cross-sectional area of the porcine skin specimens (N=3).

2.7. Statistical analysis

All quantitative data is expressed as mean ± standard deviation. Statistical analysis was performed with one-way analysis of variance (ANOVA) with Tukey significant difference post hoc test using Origin software (OriginLab Co., Northampton, MA, USA). A value of $p<0.05$ was considered statistically significant.

3. Results and discussion

3.1. Preparation of OMAs and OMA/PEG hydrogels

To prepare dual-crosslinkable OMA macromers for forming hydrogels, sodium alginates were oxidized using sodium periodate, and then methacrylate groups were introduced onto the oxidized alginate backbone using carbodiimide chemistry [22]. Oxidation of the alginate creates multiple dialdehyde groups throughout the alginate chains that enable a crosslinked network to form through relatively fast formation of imine bonds with the 8-arm PEG amines used in this study and also with amines of tissue proteins permitting adhesion [15]. The overall strategy for dual-crosslinked OMA/PEG hydrogel bioadhesive formation is showed in Figure 1. The first crosslinking networks are formed by Schiff base reaction between aldehyde groups of the OMA and amines of the 8-arm PEG and provide the cohesive force that stabilizes the bioadhesive into a hydrogel [12, 18, 26]. The second crosslinking networks formed by photocrosslinking the methacrylate groups of OMA may provide an improved resistance to shear or tensile loading and excessive swelling. It is also possible for amine groups of the 8-arm PEG to react with methacrylate groups of OMA by Michael addition reaction. However, since the Michael addition reaction rate is much slower (from hours to days) [27] when compared to the Schiff base reaction rate between amine and aldehyde groups and the photopolymerization, it likely occurs only to a minimal extent.

3.2. Gelling time of single-crosslinked OMA/PEG bioadhesives

Oscillatory rheological experiments were performed to evaluate the time to gel formation of single-crosslinked OMA/PEG bioadhesives formed with OMAs with a range of aldehyde content. OMA and PEG solutions were quickly mixed and immediately applied to the rheometer where the mixed solutions were subjected to oscillatory time sweeps. Subsequently, the kinetics of the gel formation was determined by monitoring the storage (G') and loss (G") moduli for the forming hydrogels over time. As shown in Figure 2A, both moduli for all conditions elevated as the gelation proceeded over time, indicating the formation of well-developed crosslinked three-dimensional networks. The point at which G' becomes equal to G" is typically used as a gelling time (t_{gel}) [28]. As expected, the OMA-20/PEG (t_{gel} = 4.9±0.4 min) exhibited faster gelation and higher resultant storage modulus (G') compared to the OMA-14/PEG (t_{gel} = 8.0±0.3 min) due to the larger number of aldehyde groups of OMA-20 per 8-arm PEG amine (Figure 2B). OMA-9/PEG showed the slowest gelation (t_{gel} = 25.0±4.1min) and the lowest G' since the OMA-9 had the least number of aldehyde groups available to react with the 8-arm PEG amines (Figure 2B). Control over the degree of alginate oxidation permits regulation of the gelling time of the OMA/PEG bioadhesives as well as their mechanical properties, and this allows for tailoring of these bioadhesive properties depending on the clinical application.

3.3. Rheology of the OMA/PEG bioadhesives

Rheological experiments were also performed on the single- and dual-crosslinked OMA/PEG hydrogels to examine the effects of the degree of alginate oxidation and crosslinking on the hydrogel mechanical properties. Storage moduli (G') were plotted as a function of frequency, which were significantly ($p<0.05$) higher than loss moduli (G", data not shown) at all frequencies tested for all hydrogel groups. As shown in Figure 3, the storage modulus of single-crosslinked OMA/PEG hydrogels increased with increasing alginate oxidation. This increase in storage modulus may be a result of increased aldehyde groups capable of reacting with the amines of the PEG. As the frequency increased from 0.6 to 100 rad/sec, a moderate increase of G' was observed for all single-crosslinked OMA/PEG hydrogels, indicating that the single-crosslinked OMA/PEG hydrogels are fairly viscoelastic [29], while all dual-crosslinked OMA/PEG hydrogels exhibited a plateau of G' from 0.6 to 100 rad/sec, which indicates that the hydrogels are more elastic in nature in this frequency range [30].

While there was no significant difference in G' between the dual-crosslinked OMA/PEG hydrogels, there was a trend of decreasing G' with increasing oxidation of alginate. This finding is supported by our previous work which demonstrated that G' of photocrosslinked OMA hydrogels without PEG decreased as the oxidation level increased [22]. The dual-crosslinked OMA/PEG hydrogels also exhibited significantly greater G' than the single-crosslinked OMA/PEG hydrogels at all frequencies tested. This result indicates that for the specific conditions examined in this study (i.e., concentration of 8-arm PEG amine and degree of actual methacrylation), the storage modulus of OMA/PEG hydrogels was strongly enhanced by photocrosslinking after the chemical crosslinking. Since bioadhesives may be exposed to mechanical forces (i.e., shear and tensile force) in in vivo environments [18], the increased mechanical properties of the OMA/PEG hydrogels following photocrosslinking may contribute to improving their stability when used in such applications.

Compared to G' in Figure 2A, all single-crosslinked OMA/PEG hydrogels exhibited higher G' in Figure 3. To measure the rheological properties of hydrogels, single-crosslinked OMA/PEG hydrogels were incubated for 45 min, while the gelling properties of hydrogels were measured over the course of 15 or 30 min, immediately after 30 sec mixing. The longer incubation time of single-crosslinked hydrogels prior to measurements likely increased the G' values in Figure 3 compared to G' values in Figure 2A.

3.4. Swelling kinetics, degradation profiles, and storage moduli change over time of the OMA/PEG bioadhesives

The effect of altering the degree of alginate oxidation on the single- and dual-crosslinked OMA/PEG hydrogel swelling behavior, degradation, and mechanical properties over time was examined, as these properties are important for bioadhesive functionality. As shown in Figure 4A, all single-crosslinked OMA/PEG hydrogels displayed rapid swelling kinetics. The swelling of single-crosslinked OMA-14/PEG and OMA-20/PEG hydrogels increased up to 2 and 3 days, respectively, and then rapidly decreased as the hydrogels degraded. Compared to the OMA-14/PEG and OMA-20/PEG, OMA-9/PEG hydrogels exhibited much faster swelling kinetics. The swelling of OMA-9/PEG hydrogels reached a maximum by 12 h and then rapidly decreased. All singlecrosslinked OMA/PEG hydrogels underwent complete degradation within 7 days (Figure 4B). Degradation of the single-crosslinked OMA/PEG hydrogels depended on the degree of alginate oxidation. As the alginate oxidation level increased from 9 % to 20 %, the degradation rate of the single-crosslinked OMA/PEG hydrogels decreased. Increased oxidation of the alginate creates more available aldehyde groups in the OMA to form unstable imine bonds with the free PEG amines. Increased crosslinking retards swelling and degradation until these crosslinks are hydrolyzed.

All dual-crosslinked OMA/PEG hydrogels reached equilibrium swelling rapidly within 1 day and then the dual-crosslinked OMA-9/PEG and OMA-14/PEG hydrogels gradually increased over the course of 4 weeks (Figure 4C). The equilibrium swelling ratio after 1 day increased with increasing degree of alginate oxidation. Compared to the dual-crosslinked OMA-9/PEG and OMA-14/PEG hydrogels, the swelling of the dual-crosslinked OMA-20/PEG hydrogels rapidly decreased after 2 weeks due to their almost complete degradation by 3 weeks. As shown in Figure 4D, the dual-crosslinked OMA/PEG hydrogels displayed slower degradation compared to the single-crosslinked hydrogels. Among the dual-crosslinked hydrogels, the OMA-20/PEG hydrogels exhibited the fastest degradation rate with complete degradation by 3 weeks, while the OMA-14/PEG and OMA-9/PEG hydrogels had relatively similar degradation rates, which were slower than that of OMA-20/PEG hydrogels (Figure 4D). The dual-crosslinked OMA/PEG hydrogels are expected to degrade by hydrolysis of both the alginate backbone and the two types of crosslinks in the system. The degradation profiles of photocrosslinked non-oxidized methacrylated alginate (MA)

hydrogels and photocrosslinked OMA hydrogels without PEG have been previously reported. While photocrosslinked MA hydrogels showed 33.2±1.8% mass loss by 8 weeks [31], photocrosslinked OMA hydrogels showed 75.9±3.3% to 100% mass loss by 4 weeks [22]. In this study, all OMA/PEG hydrogels single-crosslinked by imine bonds completely degraded by 1 week (Figure 4B). From these results, the unstable imine bond crosslinks between OMA and PEG likely degrade most rapidly in the dual-crosslinked hydrogels, followed by the alginate backbone and ester bonds in the photocrosslinks. Due to the similar methacrylation degree of oxidized alginates, the degradation of the dual-crosslinked OMA/PEG may be mainly affected by degree of alginate oxidation as increased oxidation can increase the alginate's susceptibility to hydrolysis [22, 32].

Changes in the storage moduli of the OMA/PEG hydrogel bioadhesives were monitored to examine the correlation between mechanical property changes and alginate oxidation level during degradation because these changes with respect to the mechanical properties and environment of the surrounding tissues can influence their success in some clinical applications [33]. Dynamic mechanical analysis was performed on the dual-crosslinked OMA-9/PEG and OMA-14/PEG hydrogels during the degradation study to quantify their storage moduli. As shown in Figure 3, there was no significant difference in initial storage moduli at day 0 between these two dual-crosslinked hydrogels (open circles and open triangles). The storage moduli of the dual-crosslinked OMA-9/PEG (Figure 4E) and OMA-14/PEG (Figure 4F) hydrogels decreased during the course of degradation and were predominantly independent of frequency. When comparing the rate of change in storage modulus, it is apparent that the storage modulus of the dual-crosslinked OMA-14/PEG hydrogels decreased more rapidly than that of the dual-crosslinked OMA-9/PEG hydrogels likely due to the higher degree swelling of the former (Figure 4C) [34].

3.5. Cytotoxicity of the OMA/PEG bioadhesives

The potential cytotoxicities of OMA and PEG macromers and dual-crosslinked hydrogels were evaluated by measuring the mitochondrial metabolic activity of hMSCs cultured on tissue culture plastic in the presence of the biomaterials using a standard MTS assay. Cell viability after 48 hrs culture was calculated by normalizing the absorbance of samples at 490 nm to that of a control without any OMA/PEG mixture, dual-crosslinked hydrogel, or insert in the medium. The viability of cells cultured in the presence of OMA/PEG mixtures and dual-crosslinked OMA/PEG hydrogels decreased as the alginate oxidation level increased (Figure 5). There was no significant difference between the mitochondrial activity of hMSCs cultured with OMA-9/PEG and OMA-14/PEG mixtures (Figure 5A), the dual-crosslinked OMA-9/PEG and OMA-14/PEG hydrogels (Figure 5B), and the dual-crosslinked OMA-14/PEG and OMA-20/PEG hydrogels (Figure 5B). Biomaterials and their degradation byproducts must be cytocompatible for biomedical applications. As determined by the MTS assay, the viability of hMSCs in monolayer culture following exposure to the OMA/PEG mixtures and dual-crosslinked OMA/PEG hydrogels was at least 67 % for the OMA-20/PEG mixtures and as high as 93 % for the dual-crosslinked OMA-9/PEG hydrogels compared to controls, which indicates a fairly cytocompatible and non-toxic nature of the hydrogel biomaterials and their degradation byproducts. The OMA-20/PEG has the highest aldehyde content, which can be toxic to cells [35] and may explain why this hydrogel group exhibited the highest cytotoxicity amongst the materials examined.

3.6. Adhesion strength of the OMA/PEG bioadhesives

Tensile tests of the single-crosslinked and dual-crosslinked hydrogels were performed to determine their adhesion strength to porcine skin and results were compared to the adhesion strength of commercially available fibrin glue. As shown in Figure 6B, the adhesion strength of single-crosslinked OMA/PEG hydrogels increased as the oxidation level of alginate

increased from 9 % to 20 %. There was no significant difference between the adhesion strength of the OMA-9/PEG hydrogels and fibrin glue. However, the OMA-14/PEG and OMA-20/PEG hydrogels exhibited significantly higher adhesion strength than fibrin glue. Since the OMA/PEG hydrogels adhere to tissue through the interaction between aldehyde groups in the bioadhesive and amine groups of tissue, controlled modulation of the OMA/PEG hydrogel aldehyde concentration could be employed to optimize the bioadhesive for various tissues, which have different amine densities [36]. To evaluate the effect of photocrosslinking on the adhesion strength of OMA/PEG hydrogels, the adhesion strength of the dual-crosslinked OMA-20/PEG hydrogels was also measured and compared with the single-crosslinked OMA-20/PEG hydrogels. The dual-crosslinked OMA-20/PEG hydrogels were chosen because they exhibit fastest gelation prior to photocrosslinking and fully degrade within 3–4 weeks, which may be more clinically applicable than the other conditions. There was no significant difference in the adhesion strength between single- and dual-crosslinked hydrogels, suggesting that the most desirable physical properties might be selected from these two types of hydrogels for a specific application without compromising adhesion strength. All bioadhesives used evaluated failed at an interface with the skin, not within the hydrogels themselves, which indicates that the hydrogel adhesion strengths were less than their fracture strengths

4. Conclusions

In this study, single- and dual-crosslinked OMA/PEG hydrogels were engineered with controllable mechanical properties, swelling ratio and degradation rates, which could be regulated by varying the degree of alginate oxidation, as biocompatible and biodegradable bioadhesives. The single- and dual-crosslinked OMA/PEG hydrogels exhibited low cytotoxicity when evaluated with hMSCs. Importantly, the adhesion strength of the OMA/PEG hydrogels, measured using porcine skin tissues, was controllable by varying the alginate oxidation level and some compositions had superior strength compared to commercially available fibrin glue. The dual-crosslinked OMA/PEG hydrogel system with tunable physical properties and adhesion strength developed in this study may be a promising bioadhesive for a wide range of biomedical applications, such as wound closure and healing, drug delivery, and biomedical device implantation.

Acknowledgments

The authors thank Shaoly M. Ahmed for research assistance, and Dr. Arnold Caplan's Skeletal Research Center Mesenchymal Stem Cell facility, especially Dr. Donald Lennon and Ms. Margie Harris, for providing the hMSCs. The authors gratefully acknowledge funding for this work from the National Institute of Arthritis and Musculoskeletal and Skin Diseases of the National Institutes of Health under Award Numbers R01AR063194 and R21AR061265.

References

1. Palacio MLB, Bhushan B. Bioadhesion: a review of concepts and applications. Philos T R Soc A. 2012; 370:2321–2347.
2. Mehdizadeh M, Yang J. Design Strategies and Applications of Tissue Bioadhesives. Macromolecular bioscience. 2012
3. Mehdizadeh M, Weng H, Gyawali D, Tang L, Yang J. Injectable citrate-based mussel-inspired tissue bioadhesives with high wet strength for sutureless wound closure. Biomaterials. 2012; 33:7972–7983. [PubMed: 22902057]
4. Harris D, Robinson JR. Bioadhesive polymers in peptide drug delivery. Biomaterials. 1990; 11:652–658. [PubMed: 2090299]

5. Vernengo J, Fussell GW, Smith NG, Lowman AM. Synthesis and characterization of injectable bioadhesive hydrogels for nucleus pulposus replacement and repair of the damaged intervertebral disc. Journal of biomedical materials research Part, B Applied biomaterials. 2010; 93:309–317.
6. Fattahi T, Mohan M, Caldwell GT. Clinical applications of fibrin sealants. J Oral Maxillofac Surg. 2004; 62:218–224. [PubMed: 14762755]
7. Hoffmann B, Volkmer E, Kokott A, Augat P, Ohnmacht M, Sedlmayr N, et al. Characterisation of a new bioadhesive system based on polysaccharides with the potential to be used as bone glue. Journal of Materials Science-Materials in Medicine. 2009; 20:2001–2009. [PubMed: 19466531]
8. Quinn, JV. Tissue adhesives in clinical medicine. 2nd ed. Hamilton: BC Decker, Inc; 2005.
9. Vauthier C, Dubernet C, Fattal E, Pinto-Alphandary H, Couvreur P. Poly(alkylcyanoacrylates) as biodegradable materials for biomedical applications. Advanced Drug Delivery Reviews. 2003; 55:519–548. [PubMed: 12706049]
10. Shalaby, SW.; Burg, KJL. Absorbable and biodegradable polymers. Boca Raton: CRC Press; 2004.
11. Furst W, Banerjee A. Release of glutaraldehyde from an albumin-glutaraldehyde tissue adhesive causes significant in vitro and in vivo toxicity. Ann Thorac Surg. 2005; 79:1522–1529. [PubMed: 15854927]
12. Artzi N, Shazly T, Baker AB, Bon A, Edelman ER. Aldehyde-Amine Chemistry Enables Modulated Biosealants with Tissue-Specific Adhesion. Adv Mater. 2009; 21:3399–3403. [PubMed: 20882504]
13. Balakrishnan B, Mohanty M, Fernandez AC, Mohanan PV, Jayakrishnan A. Evaluation of the effect of incorporation of dibutyryl cyclic adenosine monophosphate in an in situ-forming hydrogel wound dressing based on oxidized alginate and gelatin. Biomaterials. 2006; 27:1355–1361. [PubMed: 16146648]
14. Balakrishnan B, Mohanty M, Umashankar PR, Jayakrishnan A. Evaluation of an in situ forming hydrogel wound dressing based on oxidized alginate and gelatin. Biomaterials. 2005; 26:6335–6342. [PubMed: 15919113]
15. Wang DA, Varghese S, Sharma B, Strehin I, Fermanian S, Gorham J, et al. Multifunctional chondroitin sulphate for cartilage tissue-biomaterial integration. Nature Materials. 2007; 6:385–392.
16. Sharma B, Fermanian S, Gibson M, Unterman S, Herzka DA, Cascio B, et al. Human cartilage repair with a photoreactive adhesive-hydrogel composite. Science translational medicine. 2013; 5:167ra6.
17. Serrero A, Trombotto S, Bayon Y, Gravagna P, Montanari S, David L. Polysaccharide-Based Adhesive for Biomedical Applications: Correlation between Rheological Behavior and Adhesion. Biomacromolecules. 2011; 12:1556–1566. [PubMed: 21410142]
18. Artzi N, Zeiger A, Boehning F, Ramos AB, van Vliet K, Edelman ER. Tuning adhesion failure strength for tissue-specific applications. Acta Biomaterialia. 2011; 7:67–74. [PubMed: 20624496]
19. Lee Y, Chung HJ, Yeo S, Ahn CH, Lee H, Messersmith PB, et al. Thermo-sensitive, injectable, and tissue adhesive sol-gel transition hyaluronic acid/pluronic composite hydrogels prepared from bio-inspired catechol-thiol reaction. Soft Matter. 2010; 6:977–983.
20. Brigham MD, Bick A, Lo E, Bendali A, Burdick JA, Khademhosseini A. Mechanically robust and bioadhesive collagen and photocrosslinkable hyaluronic acid semi-interpenetrating networks. Tissue Eng Part A. 2009; 15:1645–1653. [PubMed: 19105604]
21. Gross M. Biological Adhesive Systems: From Nature to Technical Applications. Chemistry and Industry. 2011; 27(1)
22. Jeon O, Alt DS, Ahmed SM, Alsberg E. The effect of oxidation on the degradation of photocrosslinkable alginate hydrogels. Biomaterials. 2012; 33:3503–3514. [PubMed: 22336294]
23. Lennon DP, Haynesworth SE, Bruder SP, Jaiswal N, Caplan AI. Human and animal mesenchymal progenitor cells from bone marrow: Identification of serum for optimal selection and proliferation. In Vitro Cell Dev-An. 1996; 32:602–611.
24. Haynesworth SE, Goshima J, Goldberg VM, Caplan AI. Characterization of Cells with Osteogenic Potential from Human Marrow. Bone. 1992; 13:81–88. [PubMed: 1581112]
25. Ninan L, Monahan J, Stroshine RL, Wilker JJ, Shi RY. Adhesive strength of marine mussel extracts on porcine skin. Biomaterials. 2003; 24:4091–4099. [PubMed: 12834605]

26. Artzi N, Shazly T, Crespo C, Ramos AB, Chenault HK, Edelman ER. Characterization of Star Adhesive Sealants Based On PEG/Dextran Hydrogels. Macromolecular bioscience. 2009; 9:754–765. [PubMed: 19384975]
27. Roy A, Kundu D, Kundu KS, Majee A, Hajra A. Manganese (II) Chloride-Catalyzed Conjugated Addition of Amines to Electron Deficient Alkenes in Methanol-Water Medium. The Open Catalysis Journal. 2010; 3:34–39.
28. Chow D, Nunalee ML, Lim DW, Simnick AJ, Chilkoti A. Peptide-based Biopolymers in Biomedicine and Biotechnology. Materials science & engineering R Reports : a review journal. 2008; 62:125–155.
29. Topuz F, Okay O. Rheological Behavior of Responsive DNA Hydrogels. Macromolecules. 2008; 41:8847–8854.
30. Moura MJ, Figueiredo MM, Gil MH. Rheological study of genipin cross-linked chitosan hydrogels. Biomacromolecules. 2007; 8:3823–3829. [PubMed: 18004810]
31. Jeon O, Powell C, Ahmed SM, Alsberg E. Biodegradable, Photocrosslinked Alginate Hydrogels with Independently Tailorable Physical Properties and Cell Adhesivity. Tissue Engineering Part A. 2010; 16:2915–2925. [PubMed: 20486798]
32. Gomez CG, Rinaudo M, Villar MA. Oxidation of sodium alginate and characterization of the oxidized derivatives. Carbohyd Polym. 2007; 67:296–304.
33. Zhu J, Marchant RE. Design properties of hydrogel tissue-engineering scaffolds. Expert review of medical devices. 2011; 8:607–626. [PubMed: 22026626]
34. Anseth KS, Metters AT, Bryant SJ, Martens PJ, Elisseeff JH, Bowman CN. In situ forming degradable networks and their application in tissue engineering and drug delivery. Journal of Controlled Release. 2002; 78:199–209. [PubMed: 11772461]
35. Bassi AM, Penco S, Canuto RA, Muzio G, Ferro M. Comparative evaluation of cytotoxicity and metabolism of four aldehydes in two hepatoma cell lines. Drug and chemical toxicology. 1997; 20:173–187. [PubMed: 9292276]
36. Oliva N, Shitreet S, Abraham E, Stanley B, Edelman ER, Artzi N. Natural Tissue Microenvironmental Conditions Modulate Adhesive Material Performance. Langmuir. 2012; 28:15402–15409. [PubMed: 23046479]

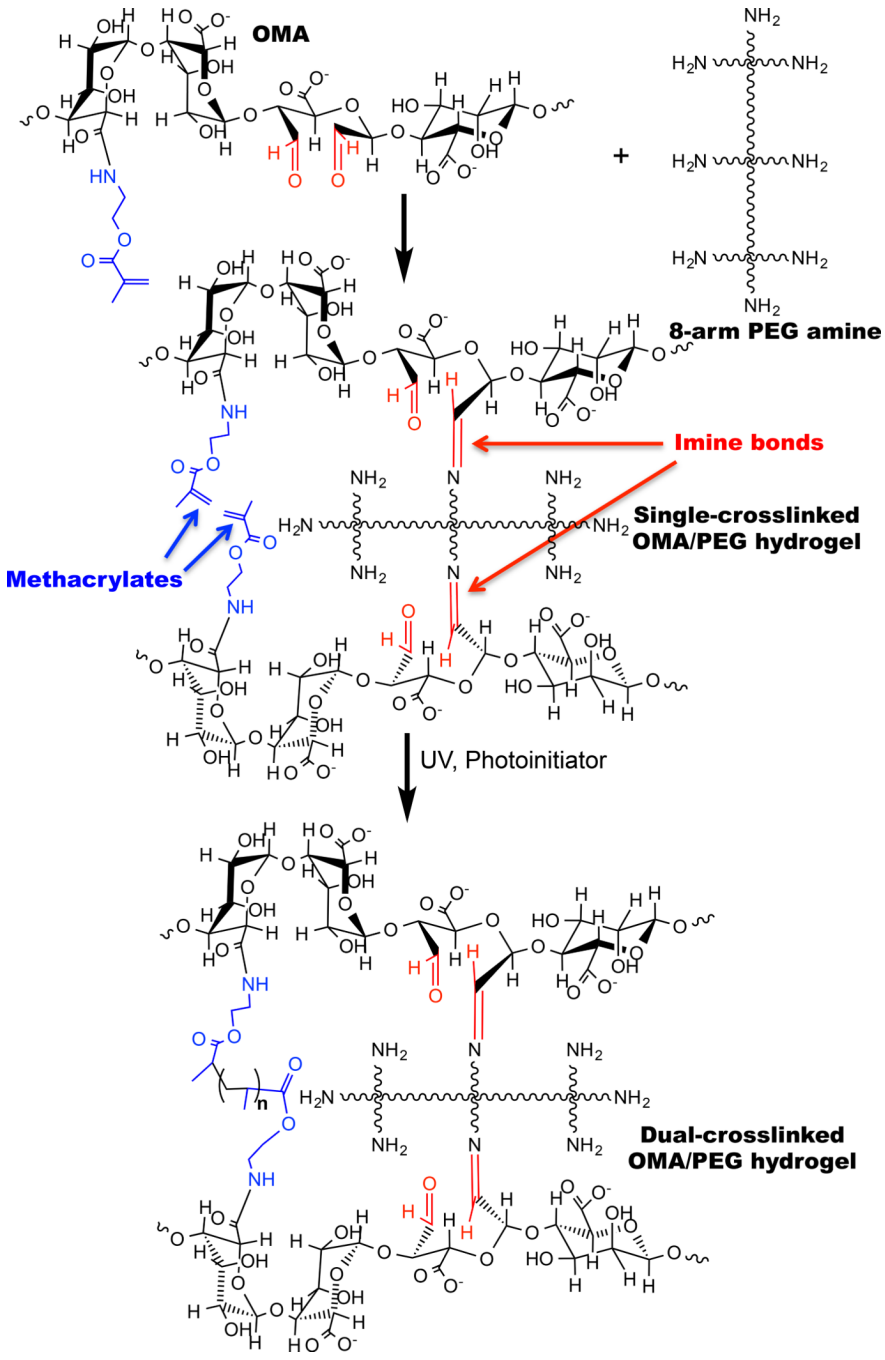

Figure 1.
Schematic illustration for preparation of single- and dual-crosslinked OMA/PEG hydrogels.

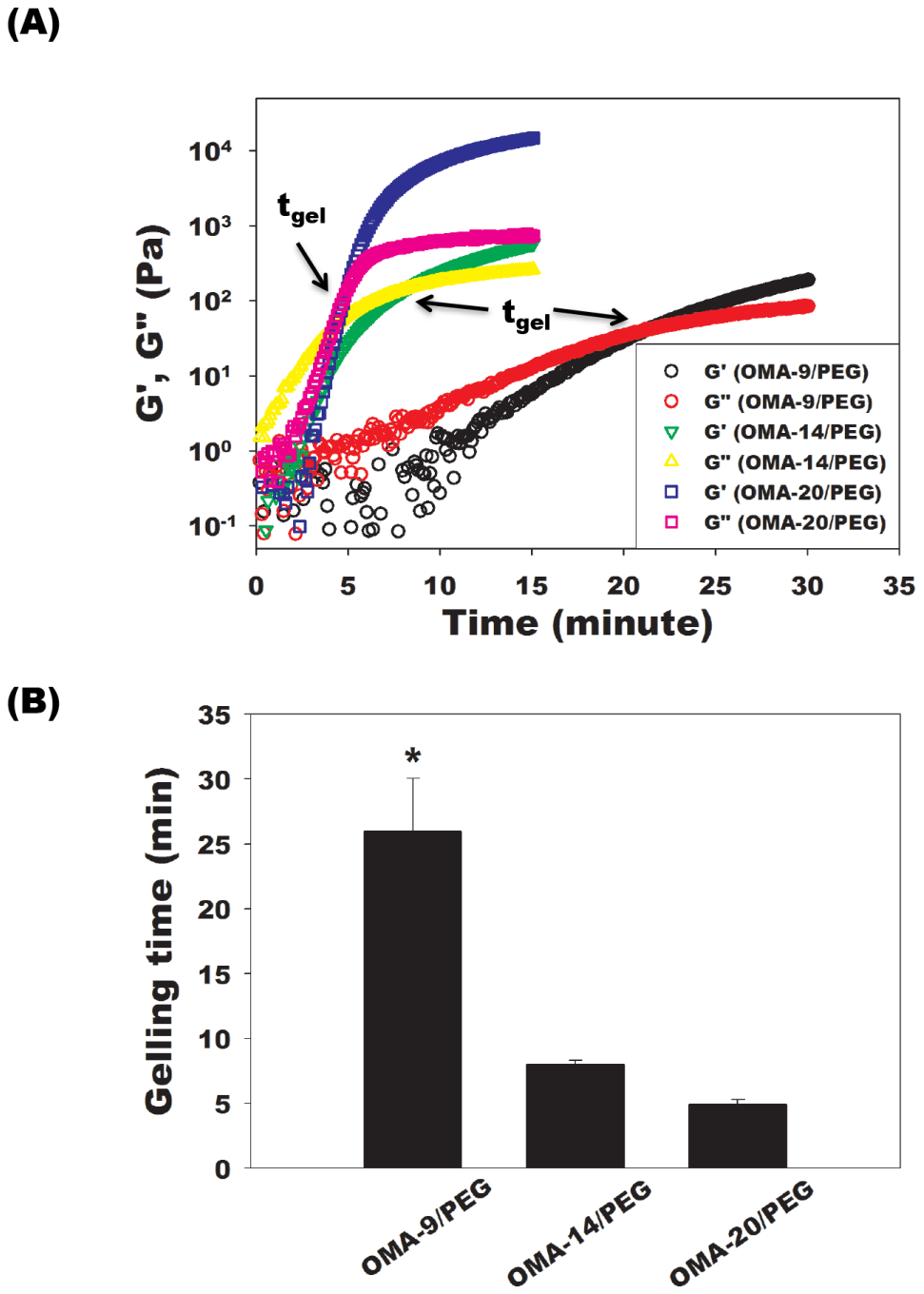

Figure 2.

(A) Representative storage moduli (G') and loss moduli (G") over time and (B) quantification of gelling time for the single-crosslinked OMA/PEG hydrogels at 25 °C. The time where G' and G" crossover occurred is denoted t_{gel} (gelling point). Values represent mean ± standard deviation (N=3). *$p<0.05$ compared with the other groups.

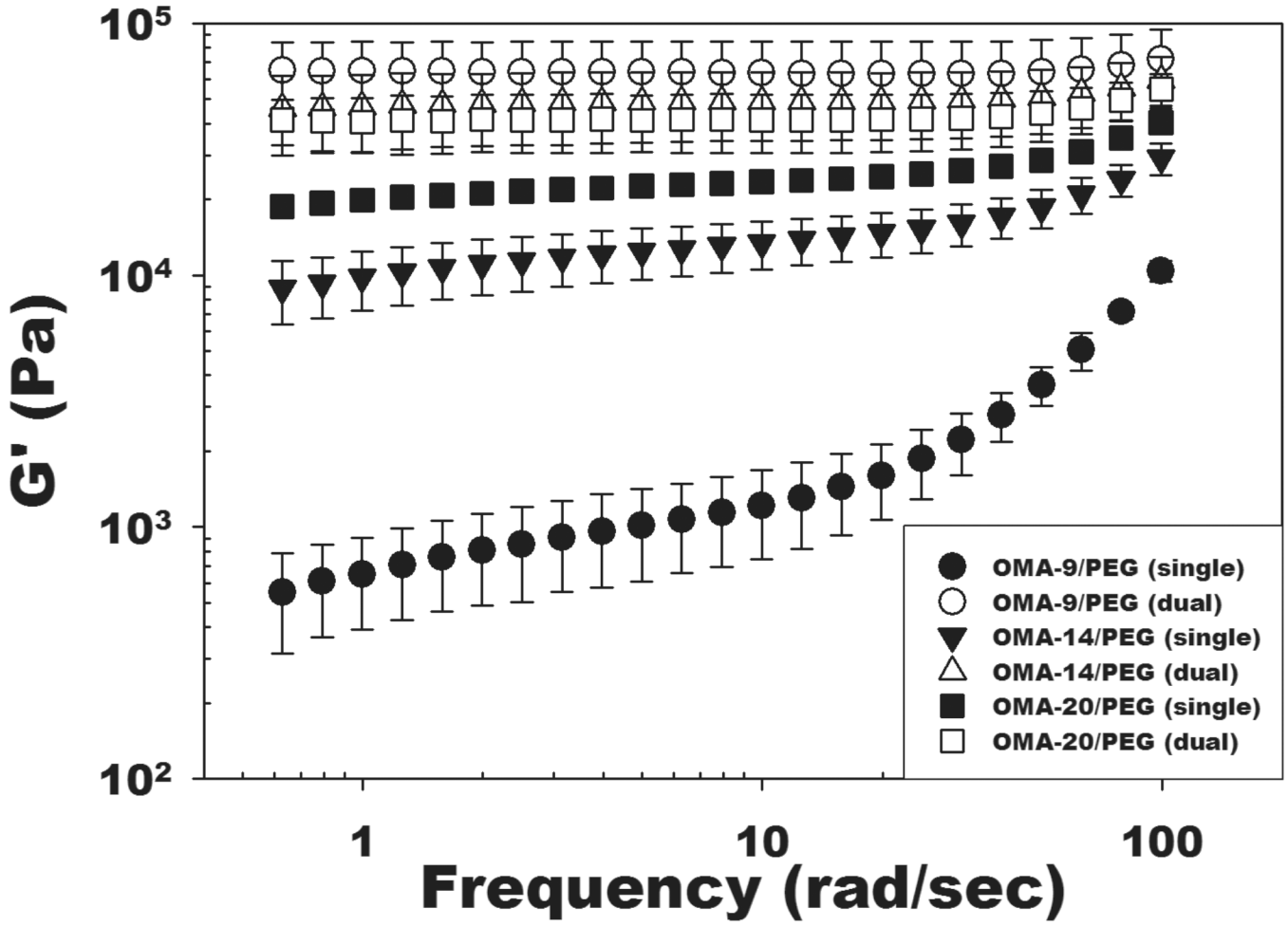

Figure 3.
Storage moduli (G') of the single- and dual-crosslinked OMA/PEG hydrogels by rheological measurements at day 0. Values represent mean ± standard deviation (N=3).

(A)

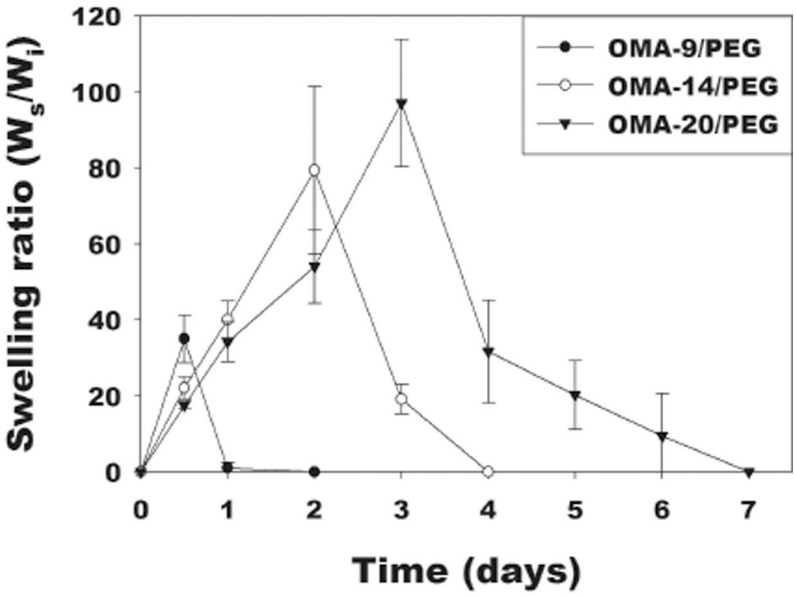

(B)

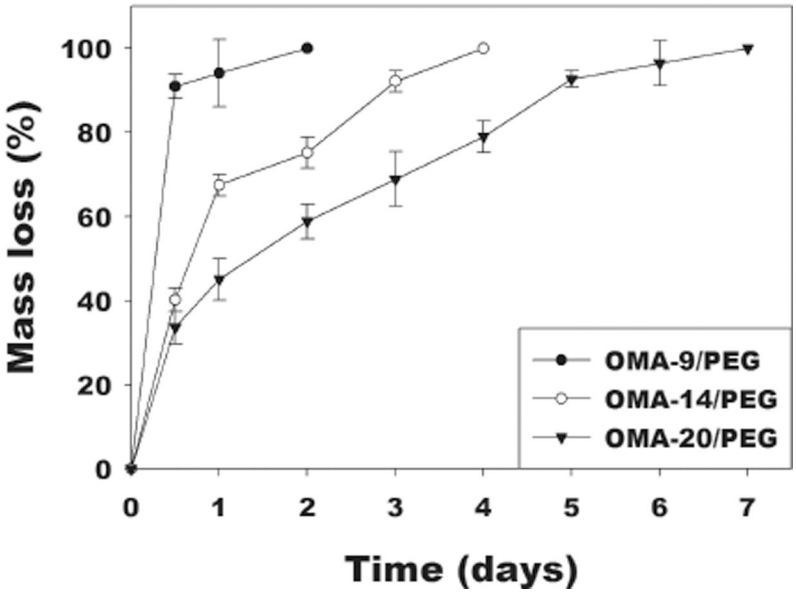

(C)

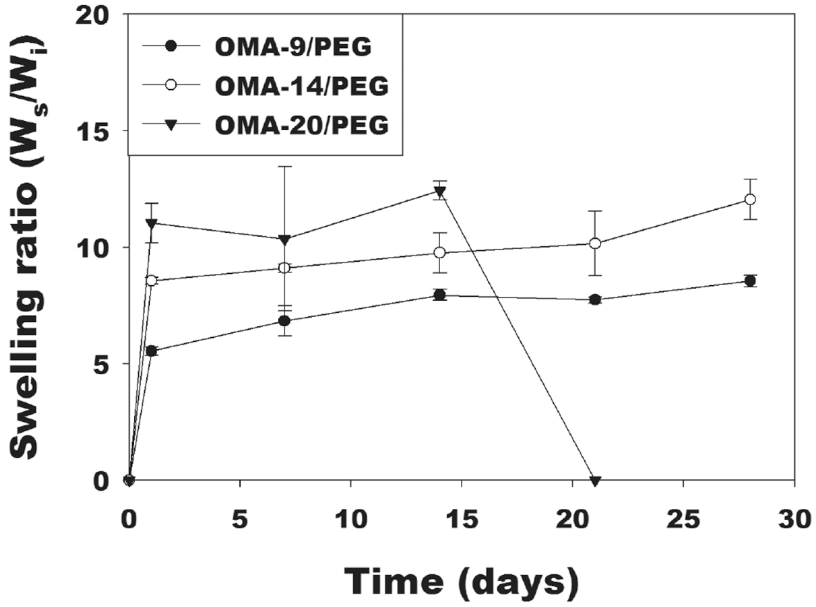

(D)

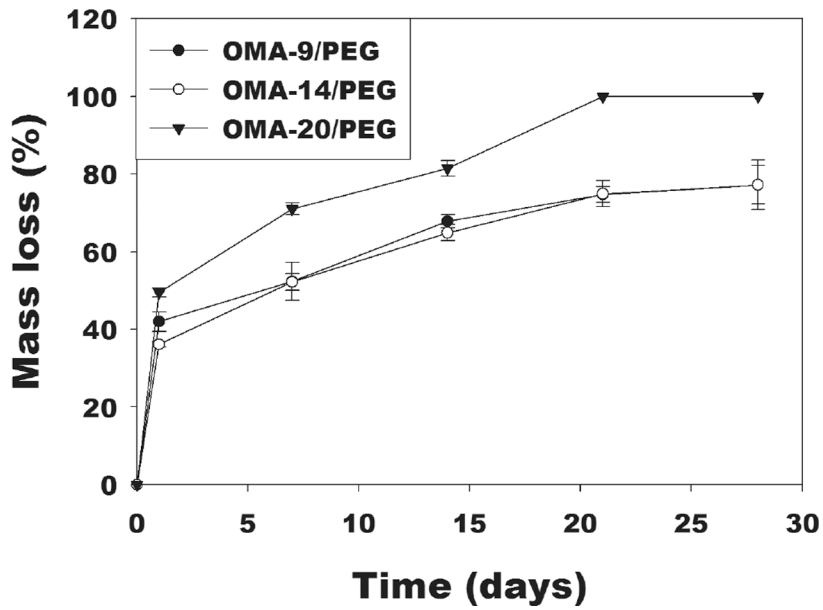

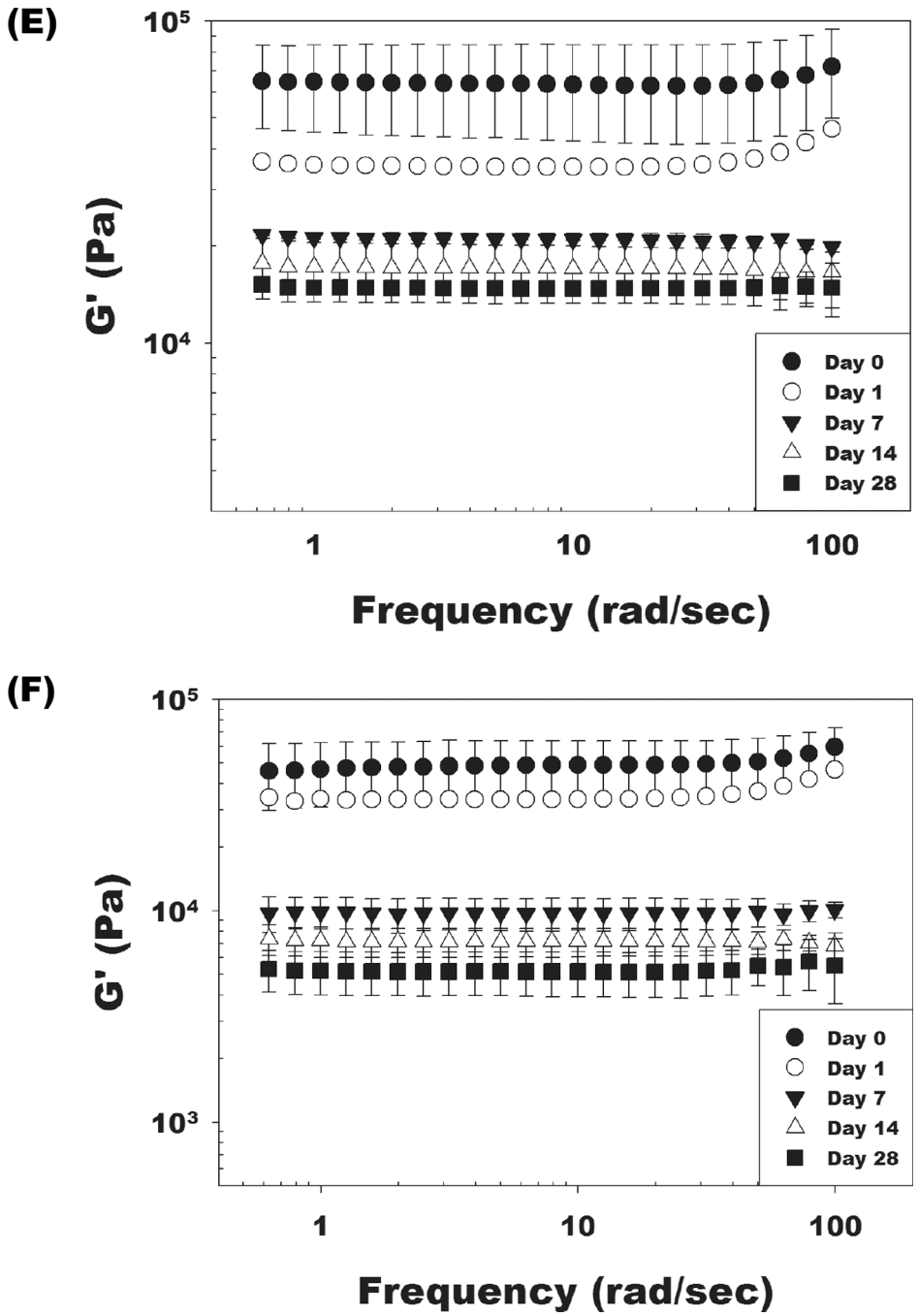

Figure 4.

Swelling ratios and mass loss of the single-crosslinked OMA/PEG hydrogels [(A) and (B), respectively] and the dual-crosslinked OMA/PEG hydrogels [(C) and (D), respectively] in DMEM over time. Storage modulus (G') changes of the dual-crosslinked (E) OMA-9/PEG and (F) OMA-14/PEG hydrogels in DMEM over time. Values represent mean ± standard deviation (N=3).

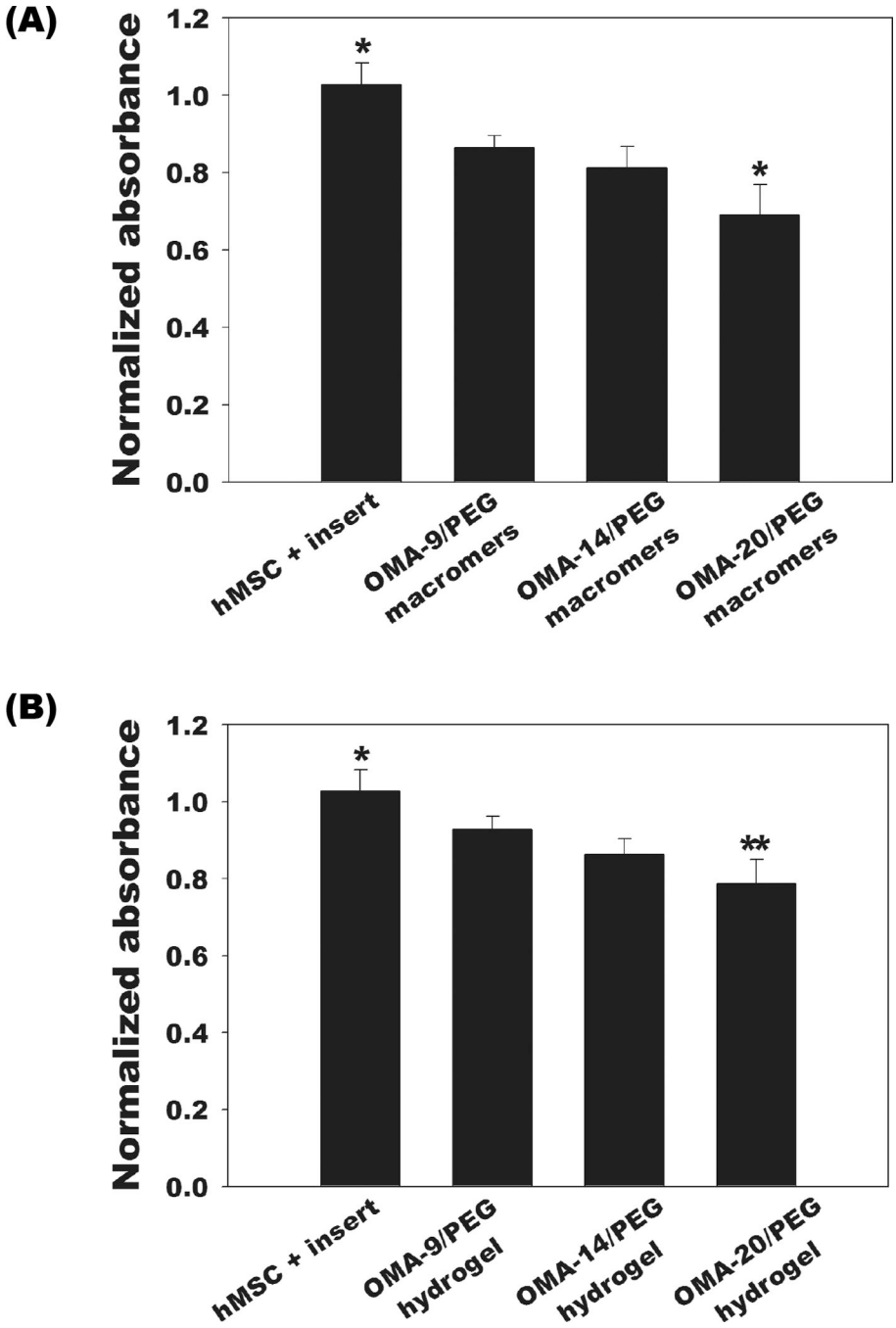

Figure 5.

Cytotoxicity of the (A) OMA/PEG mixtures and (B) dual-crosslinked OMA/PEG hydrogels on hMSCs after 48 hrs as quantified by MTS assay. The cell viability was normalized to that of a control group without any OMA/PEG mixture, dual-crosslinked hydrogel material or insert in the medium. Values represent mean ± standard deviation (N=5). *$p<0.05$ compared with the other groups. **$p<0.05$ compared with hMSC+insert and OMA-9/PEG hydrogel.

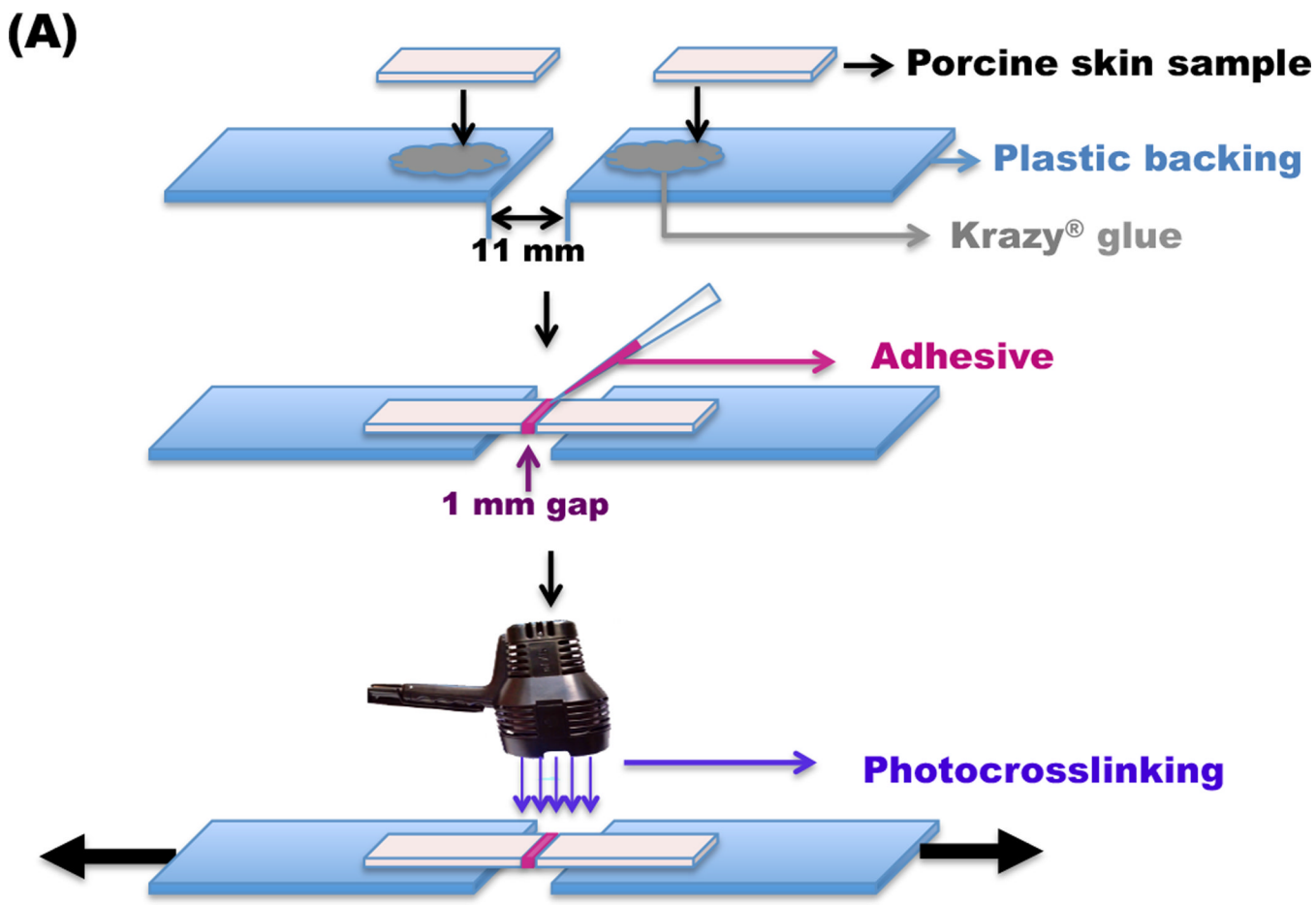

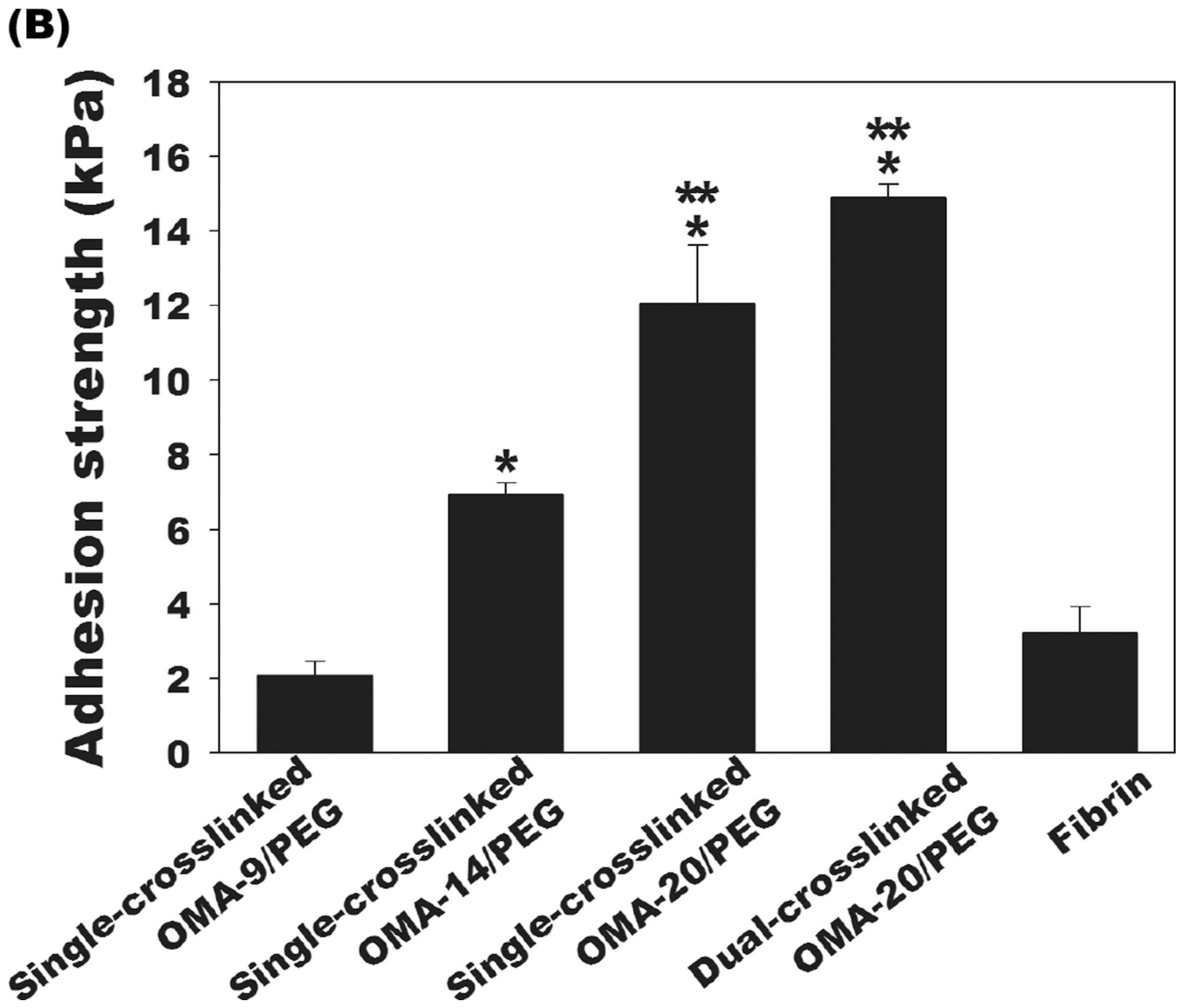

Figure 6.

(A) Schematic of the test set-up used to determine adhesion strength of OMA/PEG bioadhesives. (B) Adhesion strength of the single-crosslinked OMA/PEG bioadhesives, dual-crosslinked OMA-20/PEG bioadhesives, and fibrin. Values represent mean ± standard deviation (N=3). *$p<0.05$ compared with single-crosslinked OMA-9 and fibrin.**$p<0.05$ compared with single-crosslinked OMA-14/PEG bioadhesive.